Radiolabeling of a new nanovaccine candidate with [^{99m}Tc] TcO_4Na and [^{67}Ga] $GaCl_3$ and studying the biodistribution with in vivo molecular imaging

E.A. van Brandwijk Clinica Universidad de Navarra, Utrecht University

Article info

Keywords:
Human Serum Albumin
Nanovaccine
Molecular imaging
SPECT/CT
Stability studies
Bevacizumab
[^{99m}Tc] TcO_4Na
[^{67}Ga] $GaCl_3$

Abstract

There is a need for novel vaccinations and nanoparticles (NPs) could be appropriate candidates as nanovaccines. In vivo molecular imaging could be used to accelerate the development of new nanovaccines. To obtain these images the nanovaccine must be radiolabeled. This study aimed to optimize the radiolabeling of a new Human Serum Albumin (HSA) NP bound to bevacizumab (NPA-B) and studied the biodistribution of NPA-B in mice after subcutaneous injection. The different parameters studied for optimization of radiolabeling were: influence of decreasing the end volume on size stability, influence of adding saline to NPA-B on size, stability of NPA-B at pH 4 and stability of NPA-B during 180 min. NPA-B were double radiolabeled (bevacizumab with [^{67}Ga] $GaCl_3$; HSA NP with [^{99m}Tc] TcO_4Na) and subcutaneously administered to mice. SPECT/CT images showed activity in axillary and inguinal lymph nodes which indicates that immune cells transport NPA-B to the lymph node to initiate an immune response. In future studies bevacizumab will be replaced for S and N severe acute respiratory syndrome coronavirus (SARS-CoV-2) proteins to study the biodistribution of a novel COVID-19 vaccine.

Graphic summary

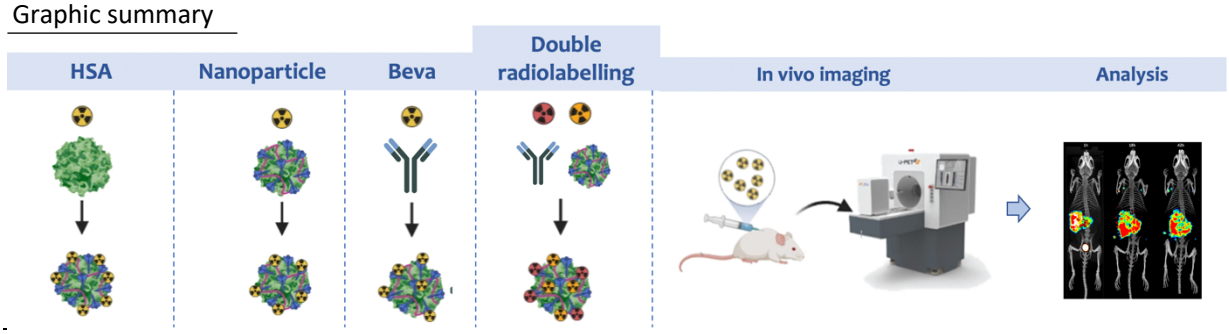

1. Introduction

Vaccination are successful in fighting diseases such as measles, mumps and polio but there are still needs for novel and effective vaccines [1][2]. For diseases as tuberculosis, malaria and acquired immune deficiency syndrome (AIDS) are no effective vaccines available. In addition many existing vaccines have disadvantages such requirement of multiple doses, difficult storage conditions and not adequately stimulating the immune system [2][3][4].

Nanoparticles (NPs) could possibly improve or overcome the problems of existing vaccines [5]. NPs are particles with a size of 10-1000 nm and can be formed out of different proteins such as human serum albumin (HSA), gelatin and lipoprotein [6]. NPs have similar size as pathogens and can thus trigger cellular and humoral immunity responses [7]. Additionally NPs can have immunogenicity and antigenicity properties and can be a slow release system which increases the antigen load [8].

A new HSA-polyethylene glycol (PEG) NP (NPA) has been developed which could be a good nanovaccine candidate. NPA can bind a protein/antigen to become a nanovaccine. The effectivity of NPA is being studied and to accelerate the development of NPA as nanovaccine, molecular imaging can be used. High-resolution micro single photon emission computed tomography/computed tomography (microSPECT/CT) can obtain information about the biodistribution of NPA in mice. This information can hardly (if possible) be obtained by any other way [9, 10].

To obtain microSPECT/CT images NPA and the protein bound to NPA must be radiolabeled. It is important to be able to make a distinction between the NPA and the protein because the biodistribution can be different. Therefore different radioisotopes could be used such as [^{99m}Tc] TcO_4Na and [^{67}Ga] $GaCl_3$.

In this study radiolabeling of NPA with bevacizumab (NPA-B) is optimized and in vivo studies in mice are performed to study the

biodistribution. The different parameters studied for optimization of radiolabeling are influence of decreasing the end volume on size stability, influence of adding saline to NPA-B on size, stability of NPA-B at pH 4 and stability of NPA-B during 180 min.

After optimization of radiolabeling, NPA-B will be double radiolabeled with [^{99m}Tc] TcO_4Na and [^{67}Ga] $GaCl_3$. First bevacizumab is radiolabeled with [^{67}Ga] $GaCl_3$. Than NPA-B are formed and NPA-B are radiolabeled with [^{99m}Tc] TcO_4Na. After double radiolabeling of NPA-B in vivo studies are performed in mice to study the biodistribution.

If radiolabeling and in vivo studies of NPA-B succeed, future research will replace bevacizumab for S and N severe acute respiratory syndrome coronavirus 2 (SARS-CoV-2) protein to form a new nanovaccine for COVID-19.

2. Material and methods

2.1 Materials and chemicals

Bevacizumab by mAbxience (León, Spain); Center for Radiopharmaceutical Sciences (CRS) kit for tricarbonyl by PSI (Villigen, Switzerland); dulbecco's Phosphate Buffered Saline (PBS) by Gibco (Bleiswijk, The Netherlands); Hydrochloric Acid 1 mol/l volumetric solution, ethanol absolute, methyl ethyl ketone (MEK) and tri-sodium citrate 2-hydrate for analysis, ACS by PanReac AppliChem ITW Reagents (Barcelona, Spain); methanol (MeOH) by CARLO ERBA (Emmendingen Germany); nitrogen extra pure 3X by PRAXAIR (Danbury, USA); p-NCS-benzyl-NODA-GA by CheMatech (Dijon, France); potassium bicarbonate, HSA and PEG 35.000 by Sigma-Aldrich (Saint Louis, USA); sodium acetate and 2,5-dihydroxybenzoate by Merck (Darmstadt, Germany); tin(II)chloride dihydrate 98% ($SnCl_2$) by Thermo Fisher Scientific Inc. (Illinois, USA); water for injections (wfi) and 0,9% NaCl by B. Braun (Kronberg, Germany)

[^{67}Ga]Ga-citrate CIS bio international 74 megabecquerel/milliliter injectable solution and Ultra-TechneKow FM 2,15-43,00 GBq generator of radionuclide by CURIUM (Saclay, France); instant thin layer chromatography – silica gel (ITLC – SG) – glass microfiber chromatography paper impregnated with silica gel by Agilent Technologies (Folsom, USA); PD midiTrap^{TM} G-25 by Cytiva (Buckinghamshire, UK); TLC Silica gel 60 by Merck (Darmstadt, Germany)

Block heater by Stuart (Staffordshire, UK); multistirrer 6 magnetic stirrer and magnet by VELP scientifica (Usmate, Italy); pH meter GLP 21+ by Crison (Barcelona, Spain); pH paper 2.0 – 9.0 by Macherey-Nagel (Dueren, Germany); rotary evaporator R300 by BUCHI (Barcelona, Spain); rotofix 32 cntrifuge by Hettich (Tuttlingen, Germany); Scan-RAM PET/SPECT radio-thin layer chromatography (TLC) scanner with LAURA software by LabLogic (Sheffield, UK); sep-pak plus light silica by Waters Corporation Milford (Massachusetts, USA); UV-3100PC spectrophotometer by VWR (Leuven, Belgium); thermo-shaker by MRC (Essex, UK); U-SPECT^6 CT E-class with mouse-collimator (UHS-M multi-pinhole M5 collimators) and MILabs software and PMOD version 4.105 by MILabs (Houten, the Netherlands); nano S90 with the zetasizer software by Malvern Panalytical (Malvern, UK)

2.2 Animals

Two-month-old and seven-month-old healthy C57/BL female mice with an average weight between 18,14 – 30,35 g were kept under controlled conditions (22 ± 5 °C with 12 hours of light/dark cycle) with free access to water and food.

The procedures involving mice were carried out in accordance with the guidelines of the European Communities Council Directive (2010/63/UE) and Spanish Government (Real Decreto 53/2013), and were approved by the Ethics Committee for Animal Experimentation of the University of Navarra (protocol 022-22).

2.3 Formation of NPA-B

Nanoparticles were prepared with the desolvation method. For the end volume of 6 ml the following method was used. Hundred mg HSA were dissolved in 7,84 ml of water for injections (wfi) under stirring. One hundred and sixty µl (4 mg) of purified bevacizumab in wfi were added and stirred for 10 minutes. The pH was adjusted with 1 M HCl to 6,4. Eight ml absolute ethanol were added with continuous flow under magnetic stirring and stirred for 10 minutes. The nanoparticles were coated with PEG 35.000 (100 mg/ml) by adding 500 µl dropwise. The solution was incubated for 30 minutes under agitation. Ethanol was removed with the rotary evaporator and an end volume of 6 ml was obtained.

After formation of the NPA-B the particle size was measured with dynamic light scattering using the nanosizer. The particle size should be

around 250 nm (C. Pangua, personal communication).

2.4 Comparison of two desalting methods

Bevacizumab is delivered in a PBS buffer. HSA tends to aggregate in the presence of salts [11]. If HSA is aggregated it is not possible to form NPs. Therefore bevacizumab should be purified into wfi. Besides the desalting method is used during radiolabeling with [^{67}Ga] $GaCl_3$ to exchange the buffer.

For the desalting PD midiTrap™ G-25 columns were used. Two desalting methods (gravity and spin protocol) were compared in their yield. Both methods were performed in duplicate.

The gravity protocol was performed by filling the column with 5 ml sodium acetate 0,25 M and the eluate was discarded. This was repeated twice. Half a mg bevacizumab was added in the column and the eluate was discarded. One and a half ml sodium acetate 0,25 M was added and the eluate was collected. The absorption was measured at 280 nm using the UV spectrophotometer.

The spin protocol was performed by filling the column with 5 ml sodium acetate 0,25 M and the eluate was discarded. This was repeated. Five ml sodium acetate 0,25 M was added again and the column was centrifuged 1000 x g for 2 minutes. The eluate was discarded. Half a mg bevacizumab was added and was eluted by centrifugation 1000 x g for 2 minutes. The elute was collected and the absorption was measured at 280 nm using the UV spectrophotometer.

2.5 The effect of decreasing the end volume of NPA-B on the size

The usual volume of subcutaneous injection in mice is 150 µl and the minimum amount of radioactivity, taking into account the acquisition time, to get good images is 2,6 MBq per mouse. NPA-B have an end volume of 6 ml therefore the radioactivity used in the experiments would be high (240 MBq), which is a safety risk for the researchers. To decrease the amount of radioactivity used during the experiments, the end volume of NPA-B were decreased (1, 2, 3, and 4 ml). The different formulations were compared in size to the standard end volume of 6 ml.

When forming NPA-B with end volumes of 1, 2, 3, and 4 ml proportionally reduced amounts of all substances were used, compared to the 6 ml end volume.

2.6 The effect of saline in a HSA solution on the stability of NPA

[^{99m}Tc] TcO_4Na is obtained from the generator using saline. When HSA is radiolabeled with [^{99m}Tc] TcO_4Na, saline is added to the formulation. HSA tends to aggregate in the presence of salts [11]. To discover at what amount of saline HSA aggregates were formed, different volumes of saline (2 ml, 200 µl, 150 µl, 100 µl, 75 µl, 70 µl, 60 µl, 50 µl, 40 µl, 30 µl, 20 µl and 10 µl) were used instead of wfi. After adding saline to the HSA in wfi, NPA-B with saline (NPA-B-s) were formed and the size was measured.

2.7 Stability over time of NPA-B-s

To test the stability of NPA-B-s during 21 hours, two formulations (end volume of 4 and 6 ml) were compared. Besides the end volume, the influence of stirring on stability was also studied. NPA-B-s were formed with an end volume of 4 and 6 ml. To mimic the addition of [^{99m}Tc] TcO_4Na, 50 µl of wfi were replaced for 50 µl of saline.

After formation of the nanoparticles the size was measured after 0, 30, 60, 90, 120 and 180 min and 21 hours. Three hours was the cutoff point because the NPA-B-s needed to be stable until administration to mice, which would not be later than 3 hours. After 21 hours the size was measured to see if the particles would be stable for 1 day.

2.8 The effect of adjusting the pH of NPA-B on the size

To radiolabel NPA-B with [^{67}Ga] $GaCl_3$ the pH is adjusted to 4. To discover whether NPA-B were stable at pH 4, the pH was adjusted using HCl in two different concentrations. HCl was added to NPA-B with two different end volumes (0,1 M in end volume of 2 ml and 1 M in end volume of 6 ml). The size of NPA-B were measured at 4 different pH's (5,5; 5,0; 4,5 and 4,0).

2.9 Comparing two methods of radiolabeling HSA with [^{99m}Tc] TcO_4Na

Radiolabeling HSA with [^{99m}Tc] TcO_4Na was performed using two methods: direct

radiolabeling using $SnCl_2$ and radiolabeling with the tricarbonyl kit.

Direct radiolabeling was performed by weighing 100 mg of HSA and dissolving it in 8 ml wfi. Samples of 1 ml were made and 40 µl of $SnCl_2$ in four different concentrations (0,1; 0,09; 0,07 and 0,05 mg/ml, respectively) were added. To prevent oxidation of $SnCl_2$, everything was performed in a nitrogen atmosphere. Thirty seven MBq [^{99m}Tc] TcO_4Na in 50 µl saline were added. The solution was incubated for 20 minutes at room temperature (RT). The quality control (QC) was performed using TLC with MEK and saline on ITLC-SG. After radiolabeling HSA, NPA-B were formed but instead of using 100 mg HSA in 8 ml, 12,5 mg [^{99m}Tc] Tc-HSA in 1 ml + 87,5 mg HSA in 7 ml were used. The particle size was measured.

Radiolabeling with the tricarbonyl kit was performed by adding 370 MBq [^{99m}Tc] TcO_4Na in 1 ml saline to the tricarbonyl kit. The kit was heated at 99 °C for 30 minutes. After cooling down, 220 µl HCl:PBS (3:2) were added and the pH was adjusted to 6,4. QC was performed with TLC using ITLC-SG and sodium citrate:MeOH (80:20). After the QC 100 µl of tricarbonyls were added to 100 mg of HSA and were incubated for 30 minutes. QC was performed with TLC using ITLC-SG and sodium citrate:MeOH (8:2). NPA-B were formed and the particle size was measured.

2.10 [^{67}Ga] $GaCl_3$ formation

To radiolabel a substance with ^{67}Ga, [^{67}Ga] $GaCl_3$ should be used. ^{67}Ga was delivered as [^{67}Ga] Ga-citrate and needed to be converted to [^{67}Ga] $GaCl_3$ using sep-pak plus light silica cartridges.

Two cartridges were coupled together. Eight ml wfi were injected in the cartridges to remove all impurities. Three hundred seventy MBq [^{67}Ga] Ga-citrate were injected in the cartridges, the elute was discarded. Five ml of wfi eliminated citrate from the cartridges, the elute was discarded. The cartridge was flushed with HCl 0,1 M and the elute ([^{67}Ga] $GaCl_3$) was collected.

2.11 Radiolabeling bevacizumab with [^{67}Ga] $GaCl_3$

To radiolabel bevacizumab with [^{67}Ga] $GaCl_3$, 6 mg (240 µl) of bevacizumab were purified in potassium bicarbonate. Twenty µl of NODAGA, in a ratio of 1:10 (HSA:NODAGA), were added and the solution was placed in a temperature controlled shaker for 40 min, with 600 rates per minute (rpm) at 37 °C. The buffer was exchanged to sodium acetate 0,25 M with 5 g/L gentisic acid. Bevacizumab-NODAGA was added to 37 MBq [^{67}Ga] $GaCl_3$ and the pH was adjusted to 4. The [^{67}Ga] Ga-NODAGA-bevacizumab ([^{67}Ga] Ga-B) solution was incubated for 30 min. After 30 minutes QC was performed with sodium citrate 1 M and ammonium acetate:MeOH (50:50) on ITLC-SG. [^{67}Ga] Ga-b was purified in wfi and NPA-B were formed. The size was measured.

2.12 Direct radiolabeling NPA-B with [^{99m}Tc] TcO_4Na

Radiolabeling of NPA-B was performed with the direct method. One ml (1,04 mg/ml) of NPA-B was labeled with [^{99m}Tc] TcO_4Na. QC was performed with MEK on ITLC-SG. The particle size was measured before and after labeling.

2.13 Double radiolabeling of NPA-B with [^{99m}Tc] TcO_4Na and [^{67}Ga] $GaCl_3$

During the in vivo studies the biodistribution of the NPA-B was studied. To make a distinction between the biodistribution of the NPs and bevacizumab, both substances were radiolabeled separately. First bevacizumab was radiolabeled with [^{67}Ga] $GaCl_3$, then NPA-B were formed and eventually NPA-B were radiolabeled with [^{99m}Tc] TcO_4Na. QC's were performed and the size was measured. Besides the size stability over 2,5 hours was studied.

2.14 In vivo biodistribution studies

During the in vivo studies 2 mice got double radiolabeled NPA-B. Bevacizumab was radiolabeled with 4 MBq [^{67}Ga] $GaCl_3$ and NPA-B were radiolabeled with 10 MBq [^{99m}Tc] TcO_4Na. Two other mice got the controls, one mouse got 4 MBq [^{67}Ga] $GaCl_3$ and one mouse got 10 MBq [^{99m}Tc] TcO_4Na.

Animals were stunned with 2% isoflurane gas before subcutaneous administration of NPA-B/control in the back. After administration the mice were quickly awakened. After 1, 18 and 42 hours the mice were placed in the mouse-collimator in the SPECT scanner under continuous anaesthesia with isoflurane (2 % in 100 % O2 gas) to acquire a whole body scan in list mode format over 30 min.

After the SPECT images, CT scans were made to obtain anatomical information using a tube setting of 55 kV and 0,33 mA.

The SPECT images were reconstructed using the ^{99m}Tc photopeak centred at 140 keV, the ^{67}Ga photopeak centred at 99, 190 and 306 keV with a 20 % energy window width and using a calibration factor to obtain the activity information (MBq/mL). Finally, attenuation correction was applied using the CT attenuation map. Studies were visualized using PMOD software. The group of images corresponding to the same animal were corrected with a numerical factor to compensate for the ^{99m}Tc and ^{67}Ga decay.

3. Results

3.1 Comparison of two desalting methods

The gravity and spin protocol were compared to establish the protocol with best yield. The absorption for both methods was equal (0,071 AU), which indicates that both methods have equal yield. The absorption was compared instead of calculating the concentration because NODAGA was probably interfering in the absorption. Therefore the concentration could not be calculated.

The spin protocol is used in further experiments because it is faster and easier.

3.2 The effect of decreasing the end volume of NPA-B on the size

As the end volume got smaller, the size of the nanoparticles got smaller (figure 1). Except for the 1 ml formulation of NPA-B which got a higher size. The polydispersity index (PDI) got slightly higher (PDI 1 ml: 0,111; PDI 6 ml: 0,100) (figure 1).

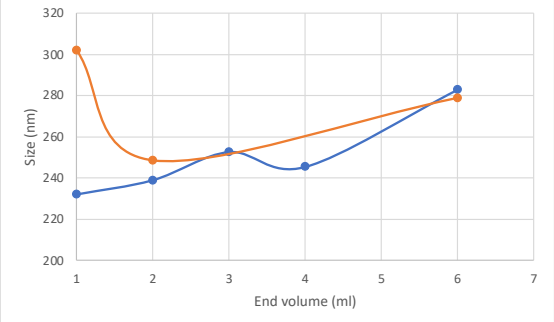

Figure 1: influence of the end volume on the NP size. Blue: NPA; orange: NPA-B.

For in vivo studies 6 ml end volume should be used because this formulation is most stable. For stability tests end volumes smaller than 6 ml could be used to save time, because of less time of rotary evaporating. In addition it saves materials.

3.3 The effect of saline in a HSA solution on the stability of NPA

After adding more than 50 µl saline in the 2 ml end volume formulation of NPA, aggregates were formed. The size of the particles increased directly after adding saline (figure 2). After adding more than 10 µl saline the size increases a lot and after adding more than 50 µl saline aggregates are formed (figure 2). The PDI was similar (0,095 for 0 µl vs 0,083 for 50 µl).

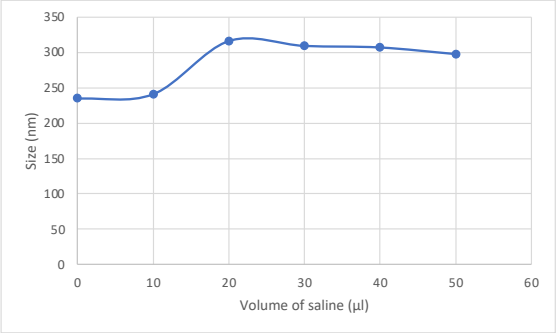

Figure 2: influence of saline volume on size of NPA with an end volume of 2 ml.

The desired activity of [^{99m}Tc] TcO_4Na should be obtained in a maximum volume of 50 µl saline.

NPA were used in this experiment in order not to waste bevacizumab. The effect of saline on NPA is probably the same as on NPA-B because saline interferes with HSA, not with bevacizumab.

3.4 Stability over time of NPA-B-s

The size of NPA-B-s formed with the 4 ml stirred formulation and the 6 ml stirred and unstirred formulation were stable for at least 180 minutes (figure 3). After 21 hours the sizes of all formulations decreased (table 1). The PDI of the stirred formulations was high and these results were thus unreliable (table 1). After 21 hours the nanoparticles were not stable anymore.

The size of NPA-B-s with an end volume of 4 ml was higher than the size of NPA-B-s with an end volume of 6 ml. This seems in contrary with the results in figure 1 but in figure 1 NPA-B were used and in figure 3 NPA-B-s were used.

Saline tends to increase the size, especially in the smaller end volume formulations.

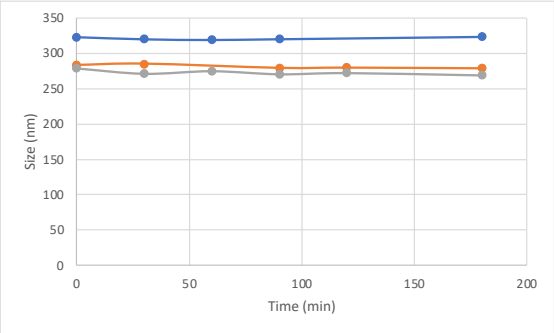

Figure 3: stability of NPA-B-s with an end volume of 4 and 6 ml during 180 min. Blue: stirred NPA-B-s 4 ml end volume; orange: stirred NPA-B-s 6 ml end volume; grey: unstirred NPA-B-s 6ml end volume.

Table 1: *size of NPA-B after 21 hours.*

Name	Size (nm)	PDI
4 ml stirred	267,3	0,248
6 ml stirred	236,7	0,228
6 ml	254,0	0,149

3.5 The effect of adjusting the pH of NPA-B on the size

The size of the particles in the 2 ml formulation increased directly (table 2). Aggregates were formed at pH 4,5. The PDI also increased (0,102 at unadjusted pH vs 0,122 at pH 5).

The size of the particles in the 6 ml formulation also increased directly (table 2). The nanoparticles fell apart at pH 4 and aggregates were formed after 1 hour at pH 4. The PDI also increased (0,100 at unadjusted pH vs 0,157 at pH 5,5 and 0,232 at pH 4,5).

It is not possible to lower the pH of NPA-B to 4, therefore it is not possible to radiolabel NPA-B with [^{67}Ga] $GaCl_3$.

Table 2: *effect of pH adjustment of NPA-B on the size.*

	NPA-B 2 ml pH corrected with HCl 0,1 M	NPA-B 6 ml pH corrected with HCl 1 M
pH not corrected	252,4 nm	278,9 nm
pH 5.5	-	312,8 nm
pH 5	279,6 nm	-
pH 4.5	Aggregates	615,7 nm
pH 4	Aggregates	Fell apart
After 1 hour	-	Fell apart and aggregates

3.6 Comparing two methods of radiolabeling HSA with [^{99m}Tc] TcO_4Na

To radiolabel HSA with [^{99m}Tc] $^{99m}TcO_4Na$ two different methods (direct radiolabeling with $SnCl_2$ and radiolabeling with tricarbonyl kit) of radiolabeling were studied to achieve the maximum percentage of [^{99m}Tc] Tc-HSA.

The first method tested was direct radiolabeling with [^{99m}Tc] TcO_4Na using 4 different concentrations of $SnCl_2$. The 0,07 mg/ml $SnCl_2$ solution resulted in the highest labeling efficiency, with 97,93% labeling efficiency in saline and 96,44% in MEK (Figure 4). It is important to have some free ^{99m}Tc to make sure ^{99m}Tc is not further reduced to a lower oxidation state. High excess of $SnCl_2$ may lead to formation of mixed metal complexes and colloid formation. This must be prevented to form good NPs.

The size of NPA-B with [^{99m}Tc] Tc-HSA were higher than the non-radiolabeled NPA-B (313,4 vs 272,4 nm). The PDI was higher for the radiolabeled NPA-B (0,135 vs 0,092).

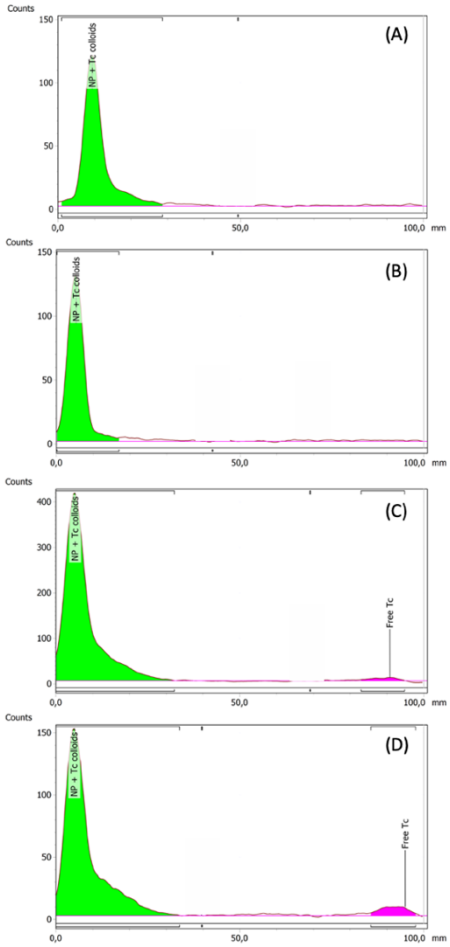

Figure 4: Radio-TLC results of radiolabeling optimalization of [^{99m}Tc] Tc-HSA with different concentrations of $SnCl_2$, QC was performed with saline on ITLC-SG. (A) 0,5 mg/ml (B) 0,1 mg/ml (C) 0,07 mg/ml (D) 0,05 mg/ml.

The tricarbonyl kit gave inconsistent results at the QC of the tricarbonyl kit. Sometimes the tricarbonyl kit worked but most of the time the QC of the tricarbonyl kit was not good. Free technetium was very high (69,16%) and the tricarbonyls were low (29,82%) (figure 5). Because the QC was inconsistent, labeling HSA with the tricarbonyl kit was not possible.

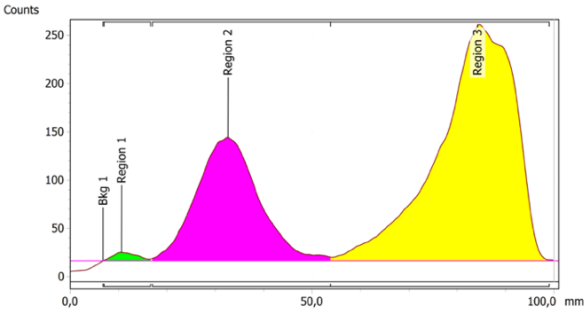

Figure 5: Radio-TLC results of the QC of the tricarbonyl kit used for radiolabeling HSA. QC was performed with sodium citrate:MeOH (50:50) on ITLC-SG. Region 1: colloids; region 2: tricarbonyls and region 3: free ^{99m}Tc.

3.7 Radiolabeling bevacizumab with [^{67}Ga] $GaCl_3$

Radiolabeling bevacizumab with [^{67}Ga] $GaCl_3$ had high efficiency (91,04% [^{67}Ga] Ga-b). There was little [^{67}Ga] Ga-NODAGA (8,96%) which was removed after purification (figure 6).

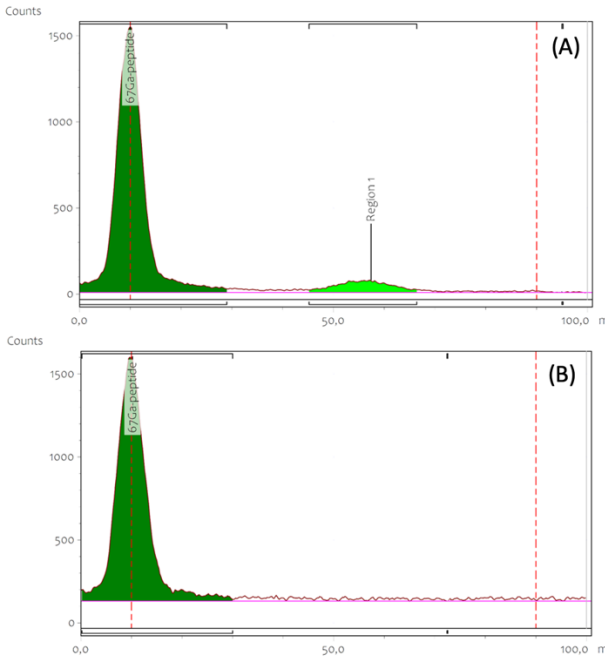

Figure 6: Radio-TLC results of [^{67}Ga] Ga-b. QC was performed with sodium citrate 1 M on ITLC-SG. 67Ga-peptide: [^{67}Ga]-b; region 1: [^{67}Ga] Ga-NODAGA. (A) before purification, 67Ga-peptides: 91,04% and region 1: 8,96%; (B) after purification, 67Ga-peptides: 100%.

The size of the nanoparticles with [^{67}Ga] Ga-b were slightly smaller than the non-radiolabeled nanoparticles (263,5 vs 272,4 nm). The PDI was similar (0,094 vs 0,092).

3.8 Direct radiolabeling NPA-B with [^{99m}Tc] TcO_4Na

The results were similar to figure 4. The 0,07 mg/ml $SnCl_2$ solution resulted in the highest labeling efficiency (98,35% in MEK). The size of [^{99m}Tc] Tc-NPA-B were similar to the size of NPA-B (278,7 vs 272,4 nm). The PDI was higher for [^{99m}Tc] Tc-NPA-B (0,129 Vs 0,092).

3.9 Double radiolabeling of NPA-B with [^{99m}Tc] TcO_4Na and [^{67}Ga] $GaCl_3$

After formation of NPA-B with [^{67}Ga] Ga-b, QC was performed with sodium citrate 1 M on ITLC-SG. At t=0 there was free ^{67}Ga (10,69%). The QC was repeated after 90 min. At t=90 the free ^{67}Ga was reduced to 5,76% (figure 7).

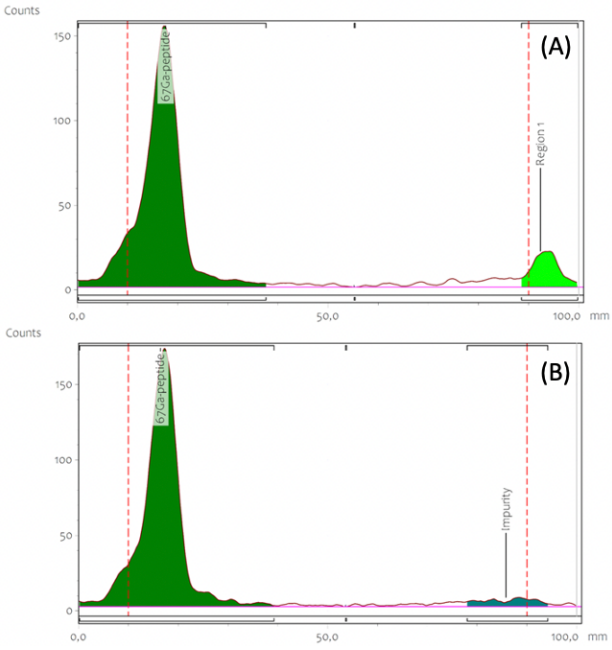

Figure 7: Radio-TLC results of NPA-B with [^{67}Ga] Ga-b. QC was performed with sodium citrate 1 M on ITLC-SG. 67Ga-peptide: [^{67}Ga] Ga-b; region 1/impurity: ^{67}Ga. (A) t=0 min 67Ga-peptides: 89,31% and region 1: 10,69%; (B) t=90 min 67Ga-peptides: 94,24% and impurity 5,76%.

After double radiolabeling of NPA-B, QC was performed with saline on ITLC-SG. There was free ^{99m}Tc and free ^{67}Ga (figure 8).
The QC in figure 8 was performed in saline. Both ^{99m}Tc and ^{67}Ga were in the sample. For ^{67}Ga the QC should have been performed with sodium

citrate 1 M. After running the strips in saline and sodium citrate 1 M, they should have been read in the gamma counter to make a distinction between ^{99m}Tc and ^{67}Ga. This was not performed thus figure 8 is not very useful.

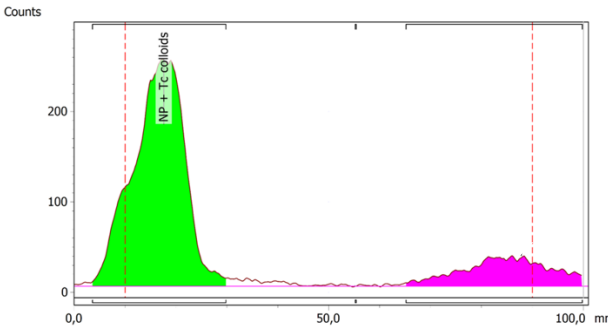

Figure 8: Radio-TLC results of [^{99m}Tc] Tc-NPA-B with [^{67}Ga] Ga-B. QC was performed with saline on ITLC-SG. Green (double radiolabeled NPA-B): 80,66%; pink (free ^{99m}Tc and free ^{67}Ga]): 19,34%.

The size of [^{99m}Tc] Tc-NPA-B with [^{67}Ga] Ga-b were smaller than non-radiolabeled NPA-B (251,7 nm vs 272,4 nm). The PDI was lower (0,082 vs 0,092).

The size of NPA-B with [^{67}Ga] Ga-b and [^{99m}Tc] Tc-NPA-B with [^{67}Ga] Ga-b decreased slightly over 2,5 hours, which indicates that the stability was good (figure 9). The PDI increased (0,094 vs 0,118 for NPA-B with [^{67}Ga] Ga-b and 0,082 vs 0,100 for [^{99m}Tc] Tc-NPA-B with [^{67}Ga] Ga-b). [^{99m}Tc] Tc-NPA-B with [^{67}Ga] Ga-b were measured at 1,5 hours because the particles were labeled with [^{99m}Tc] TcO_4Na after 1,5 hours, after formation of the NPA-B with [^{67}Ga] Ga-b.

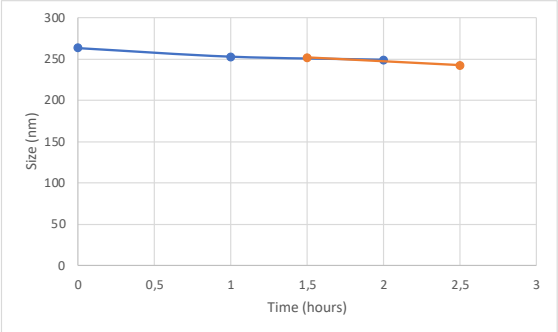

Figure 9: stability over 2,5 hours of (double) radiolabeled NPA-B. Blue: NPA-B with [^{67}Ga] Ga-b; orange: [^{99m}Tc] Tc-NPA-B with [^{67}Ga] Ga-b.

3.10 In vivo biodistribution studies

Two mice (30,15 - 30,35 g) got 150 µl of double radiolabeled NPA-B. [^{67}Ga] Ga-b had an activity of 4,13 MBq and [^{99m}Tc] Tc-NPA-B had an activity of 9,66 MBq. Two other mice got the controls, one mouse (18,14 g) got 5,33 MBq [^{67}Ga] $GaCl_3$ and one mouse (18,81 g) got 8,10 MBq [^{99m}Tc] TcO_4Na.

Control [^{99m}Tc] TcO_4Na

One hour after subcutaneous injection there was activity at the side of injection, bladder, stomach, intestine, thyroid, nose and in the salivary glands (figure 10 and 11). After 18 hours there was activity at the side of injection, stomach, intestine and salivary glands (figure 10 and 11).

[^{99m}Tc] TcO_4Na is probably excreted via the kidneys because there is activity in the bladder.

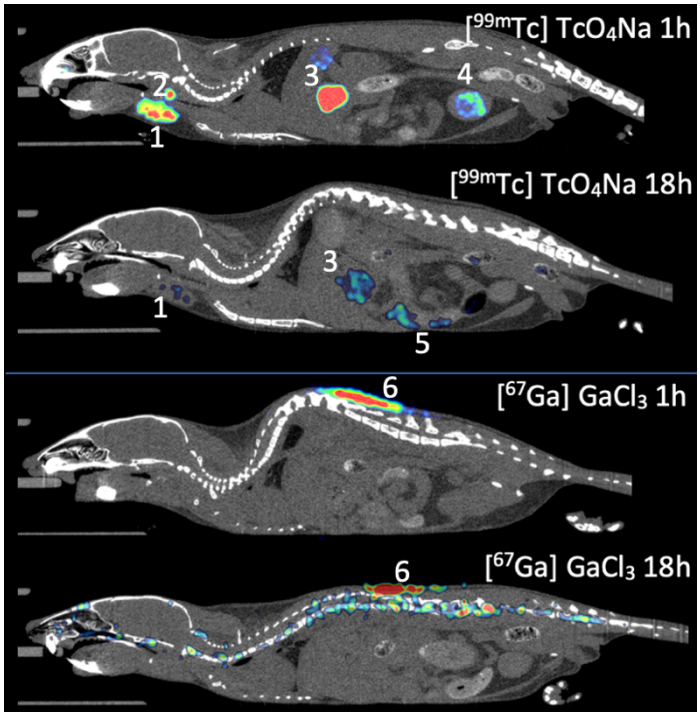

Figure 10: SPECT/CT images of the subcutaneous biodistribution of [^{99m}Tc] TcO_4Na and [^{67}Ga] $GaCl_3$. 1: salivary gland; 2: thyroid; 3: stomach; 4: bladder; 5: intestine and 6: injection side.

Control [^{67}Ga] $GaCl_3$

One hour after injection there was activity at the side of injection. After 18 hours there was activity in the bone marrow and probably activity in soft tissue (figure 10 and 11).

[^{99m}Tc] Tc-NPA-B with [^{67}Ga] Ga-b

One hour after subcutaneous injection there was activity of ^{99m}Tc at the side of injection, bladder, and renal cortex (figure 12 and 13). ^{67}Ga had activity at the side of injection.

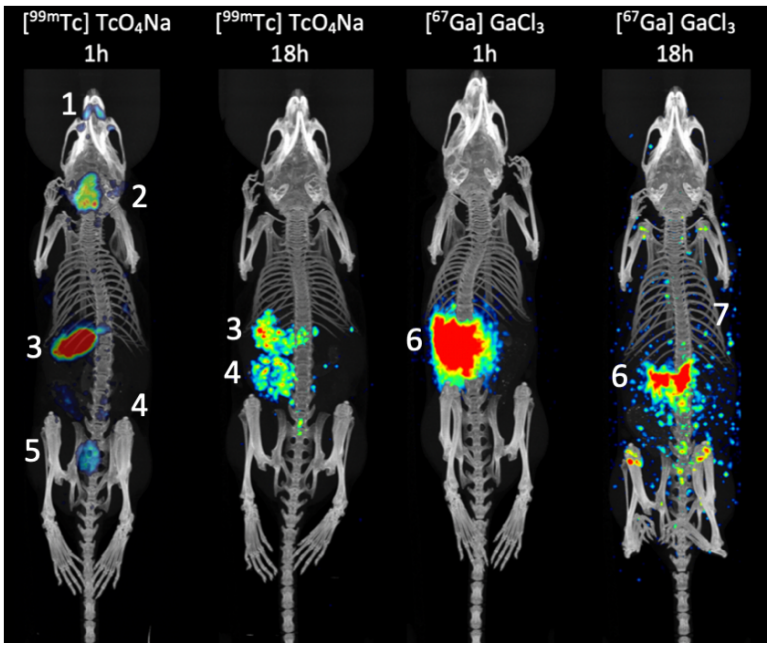

Figure 11: SPECT/CT 3D images of the subcutaneous biodistribution of [^{99m}Tc] TcO_4Na and [^{67}Ga] $GaCl_3$. 1: nose; 2: salivary gland and thyroid; 3: stomach; 4: intestine; 5: bladder; 6: side of injection and 7: soft tissue (all the small dots).

After 18 hours there was activity at the side of injection, in the axillary and inguinal lymph nodes of both ^{99m}Tc and ^{67}Ga (figure 13, 14 and 15).

After 42 hours there was activity of ^{67}Ga at the side of injection, in the axillary and inguinal lymph nodes (figure 13). There was no activity of ^{99m}Tc because it had decayed.

As opposed to the [^{99m}Tc] TcO_4Na and [^{67}Ga] $GaCl_3$ controls there was no activity in the stomach, intestine, thyroid, nose, salivary glands and bone marrow.

Figure 12: SPECT/CT image of subcutaneous biodistribution of [^{99m}Tc] Tc-NPA-B with [^{67}Ga] Ga-b. ^{99m}Tc activity in the renal cortex.

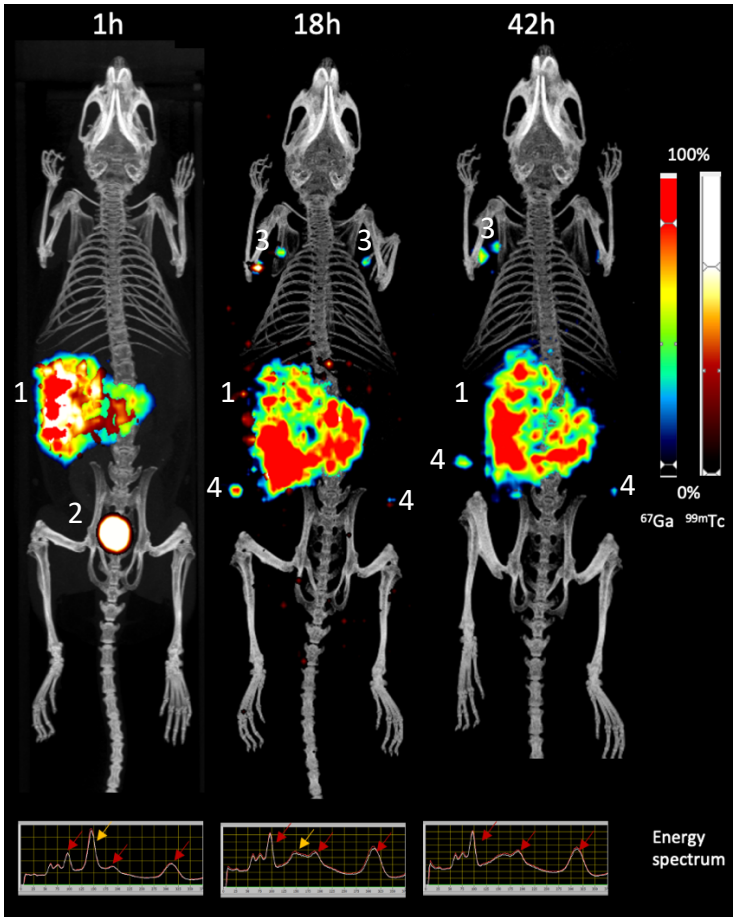

Figure 13: SPECT/CT 3D images of the subcutaneous biodistribution of [^{99m}Tc] Tc-NPA-B with [^{67}Ga] Ga-b. 1: side of injection; 2: bladder; 3 axillary lymph nodes and 4: inguinal lymph nodes.

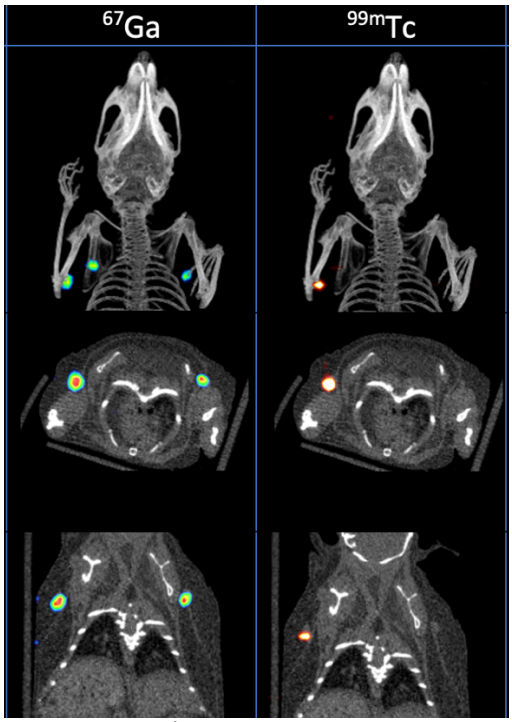

Figure 14: SPECT/CT images of axillary lymph nodes after subcutaneous administration of [^{99m}Tc] Tc-NPA-B with [^{67}Ga] Ga-b after 18 hours.

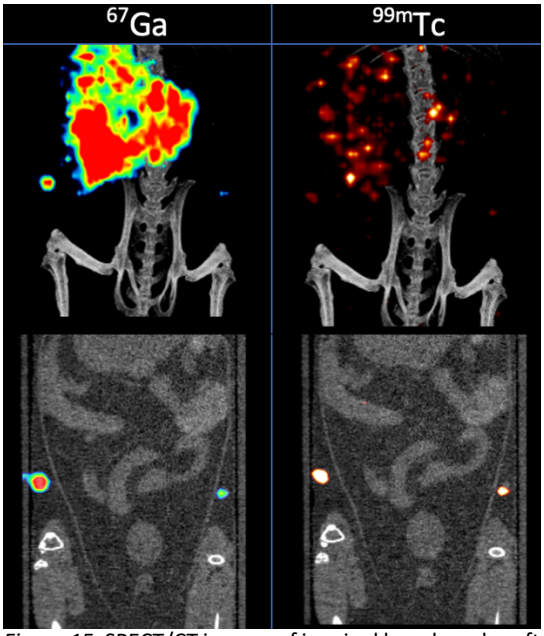

Figure 15: SPECT/CT images of inguinal lymph nodes after subcutaneous administration of [^{99m}Tc] Tc-NPA-B with [^{67}Ga] Ga-b after 18 hours.

4. Discussion

Interpretation of the results

To obtain nanoparticles with high stability, NPA-B with an end volume of 6 ml should be used and [^{99m}Tc] TcO_4Na should be added in a maximum volume of 50 µl of saline. When the end volume is smaller or the volume of saline is higher the nanoparticles will aggregate fast. The 6 ml formulation of NPA-B is stable ex vivo for at least 180 min. Administration to mice of the NPA-B should be within 180 min after formation of the NPA-B.

To radiolabel NPA-B two different radioactive substances were used: [^{99m}Tc] TcO_4Na and [^{67}Ga] $GaCl_3$. Different parts of the NPA-B were radiolabeled.

It was not possible to radiolabel NPA-B with [^{67}Ga] $GaCl_3$ because it was not possible to lower the pH of NPA-B to 4, which is needed for radiolabeling with [^{67}Ga] $GaCl_3$. At pH 4 NPA-B were aggregated.

HSA was successfully radiolabeled with [^{99m}Tc] TcO_4Na with 0,07 mg $SnCl_2$. But the size of NPA-B formed with [^{99m}Tc] Tc-HSA were higher than NPA-B. It could be possible that the biodistribution is different because of the different size. Therefore NPA-B formed with [^{99m}Tc] Tc-HSA were not used for in vivo studies.

Bevacizumab was successfully radiolabeled with [^{67}Ga] $GaCl_3$. The size of the NPA-B with bevacizumab [^{67}Ga] $GaCl_3$ were similar to the non-radiolabeled NPA-B. The bond between bevacizumab and [^{67}Ga] $GaCl_3$ was stable for at least 90 min. Free [^{67}Ga] $GaCl_3$ was smaller after 90 min than after 0 min. This could be explained because there was probably free NODAGA where the free [^{67}Ga] $GaCl_3$ had bound to. Therefore the free [^{67}Ga] $GaCl_3$ was smaller after 90 min than after 0 min.

NPA-B was successfully radiolabeled with [^{99m}Tc] TcO_4Na. The radiolabel efficiency was best with 0,07 mg/ml $SnCl_2$ concentration. The size of the radiolabeled NPA-B were similar to the non-radiolabeled NPA-B.

To radiolabel NPA-B in two different ways, bevacizumab was radiolabeled with [^{67}Ga] $GaCl_3$ and NPA-B was radiolabeled with [^{99m}Tc] TcO_4Na. The size of the double radiolabeled NPA-B was smaller than the non-radiolabeled NPA-B. The size of the double radiolabeled NPA-B was close to the reference size (250 nm).

After double radiolabeling of NPA-B, the NPA-B were administered to mice. Two controls, [^{99m}Tc] TcO_4Na and [^{67}Ga] $GaCl_3$, were also administered to mice.

The [^{99m}Tc] TcO_4Na control had activity at the side of injection, bladder, stomach, intestine, thyroid, nose and in the salivary glands. According to literature the biodistribution of [^{99m}Tc] TcO_4Na is indeed in these places. TcO_4^- is actively transported via the sodium/iodide symporter into thyroid follicular cells [12][13]. TcO_4^- is physiological absorbed in the nose and salivary glands [12]. In the stomach TcO_4^- is absorbed and excreted by either parietal cells or mucous cells, most evidence points to the mucin-secreting cells [14][15]. TcO_4^- is excreted through the kidney via glomerular filtration [16].

The [^{67}Ga] $GaCl_3$ control had activity at the side of injection, in soft tissue and in the bone marrow. According to literature ^{67}Ga distributes, after intravenous injection, evenly in soft tissues, liver, bone and it might be possible that white blood cells bind and transport ^{67}Ga. Around 90% of ^{67}Ga is bound to transferrin in the blood plasma because ^{67}Ga is a trivalent metal and acts the same as ferric ion in the body [17]. The results are not entirely similar to literature but the administration route used in literature is not subcutaneous.

After 1 hour of subcutaneous injection double radiolabeled NPA-B had activity at the side of injection, both from ^{99m}Tc and ^{67}Ga.

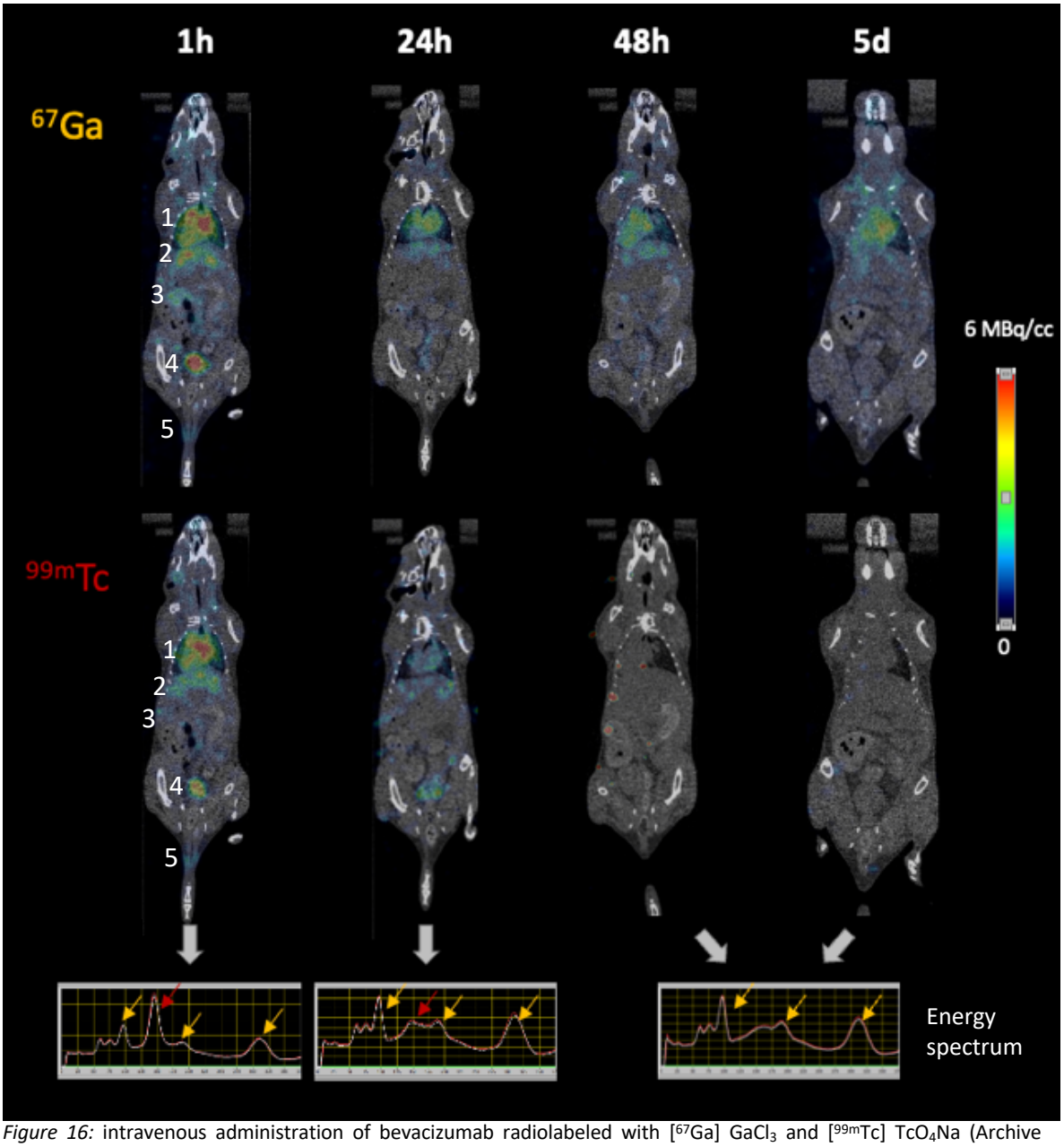

Figure 16: intravenous administration of bevacizumab radiolabeled with [^{67}Ga] $GaCl_3$ and [^{99m}Tc] TcO_4Na (Archive microSPECT lab Clinica Universidad de Navarra, 2021). 1: heart; 2: liver; 3: intestine; 4: bladder and 5: side of injection.

Besides there was activity of ^{99m}Tc in the bladder and renal cortex. According to literature a significant amount of HSA is filtered and reabsorbed by the renal tubules [18]. HSA is reabsorbed by multiligand receptors megalin and cubilin located in the proximal tubules [18][19]. The proximal tubules is located in the renal cortex. This explains why there was activity of ^{99m}Tc in the cortex. Not all HSA is reabsorbed, a part is excreted via urine [19]. Therefore there was activity in the bladder.

After 18h there was activity of ^{67}Ga in 5 lymph nodes (3 axillary and 2 inguinal lymph nodes) and in 3 of these 5 lymph nodes there was also activity of ^{99m}Tc. The activity in the lymph nodes is mostly on the left side. This can be explained because the dose is administered on the left side and substances travel through lymph vessels to the closest lymph node. The activity in the lymph nodes indicates that immune cells transport NPA-B to the lymph node to initiate an immune response. Because there is activity of both ^{99m}Tc and ^{67}Ga bevacizumab probably remains bound to the nanoparticle. Previous research of the biodistribution of intravenous bevacizumab showed activity in the liver and heart (figure 16). Figure 13, 14 and 15 do not have activity in the heart and liver which indicates that bevacizumab is not free available in the body and thus is bound to the NPA.

The double radiolabeled NPA-B is stable in vivo because unlike the controls there was no activity in the stomach, intestine, thyroid, nose, salivary glands and bone marrow.

Limitation:

When NODAGA binds to the recognition side of bevacizumab it could alter its biological activity and change the biodistribution. The chance of NODAGA binding to the recognition side is small because bevacizumab is bigger than NODAGA (149.000 Da [20] vs 593,15 Da [21]) and the recognition side of bevacizumab is small in comparison to the entire protein. Besides there are only 1-2 molecules NODAGA per molecule bevacizumab.

It is possible that the radiolabeling procedure has influence on the conformation of bevacizumab and thus possible alter the biodistribution. It would be interesting to perform SDS-PAGE and Western Blott to study the stability of the proteins after radiolabeling.

When labeling NPA-B with [^{99m}Tc] TcO_4Na, ^{99m}Tc might also bind non-specific to bevacizumab. It is not sure, on the images, whether the ^{99m}Tc is coupled to the NPA or to the bevacizumab. The chance of ^{99m}Tc binding to bevacizumab is small because the amount of bevacizumab is <4% (4 vs 100 mg) of the amount of HSA.

The images of 18h with ^{99m}Tc had low activity because of the decay of ^{99m}Tc. There is a lot of noise in the image what could lead to misinterpretation of the results.

In this research few mice were used which could lead to a low power. It could be that the results are a coincidence.

Suggestion follow-up research

A control of [^{99m}Tc] Tc-HSA could be interesting to understand the biodistribution of HSA. It is than possible to see whether the biodistribution of the HSA in NPA-B is different than the biodistribution of HSA.

The stability of bevacizumab should be studied using SDS-PAGE and Western Blott to see whether radiolabeling influences protein conformation.

NPA should be formed with the S and N SARS-CoV-2 protein. The S and N SARS-CoV-2 protein should be labeled with [^{67}Ga] $GaCl_3$ and then the NPA should be formed and labeled with [^{99m}Tc] TcO_4Na. In vivo studies should be performed.

The route of administration researched was subcutaneous. In previous research oral administration was not effective. It could be interesting to investigate whether nasal administration is effective because nasal administration is easier and more accepted than subcutaneous administration.

5. Conclusion

The optimal circumstances to radiolabel NPA-B is by using the formulation with an end volume of 6 ml. First bevacizumab should be radiolabeled with [^{67}Ga] $GaCl_3$ and be purified in wfi. Then the NPA-B should be formed. Lastly the NPA-B should be radiolabeled with [^{99m}Tc] TcO_4Na, in a maximum volume of 50 µl and using 0,07 mg/ml $SnCl_2$. The [^{99m}Tc] Tc-NPA-B with [^{67}Ga] Ga-b should be administered within three hours after formulation.

The in vivo studies showed activity in the axillary and inguinal lymph nodes after 18 and 42 hours which indicates immune cells have transported NPA-B to the lymph node to initiate an immune response. NPA might be a suitable candidate as nanovaccine but further research should be performed.

References

[1] CBG. Vaccinaties. [Internet]. Available from: https://www.cbg-meb.nl/onderwerpen/medicijninformatie-vaccinaties. [Accessed 27-06-22].
[2] Wilson-Welder JH, Torres MP, Kipper MJ, Mallapragada SK, Wannemuehler MJ, Narasimhan B. Vaccine adjuvants: Current challenges and future approaches. J. Pharm. Sci. 2009 April; 98 (4): 1278-1316.
[3] Siegrist CA. The Challenges of Vaccine Responses in Early Life: Selected Examples. J. Comp. Pathol. 2007 July; 137 (1): S4-S9.
[4] Cheng D, Kristensen D. Opportunities and challenges of developing thermostable vaccines. Expert Rev Vaccines. 2009 May; 8 (5): 547-557.
[5] Hayat SMG, Darroudi M. Nanovaccine: A novel approach in immunization. J. Cell. Physiol. 2018 December 20; 234: 12530-12536.
[6] Hong S, Choi DW, Kim HN, Park CG, Lee W, Park HH. Protein-Based Nanoparticles as Drug Delivery Systems. Pharmaceutics. 2020 July; 12 (7): 604.
[7] Kim J, Archer PA, Thomas SN. Innovations in lymph node targeting nanocarriers. Semin Immunol. 2021 August; 56: 101534.
[8] Kolachala VL, Henriquez OA, Shams S, Golub JS, Kim Y, Laroui H, Torres-Gonzalez E, Brigham KL, Rojas M, Bellamkonda RV, Johns MM. Slow-release nanoparticle-encapsulated delivery system for laryngeal injection. Laryngoscope. 2010 May; 120 (5): 988-994.
[9] Pastor Y, Larrañeta E, Erhard A, Quincooces G, Peñuelas I, Irache JM, et al. Dissolving Microneedles for Intradermal Vaccination against Shigellosis. 2019 October; 7: 159.
[10] Sánchez-Martínez M, da Costa Martins R, Quincoces G, Gamazo C, Caicedo C, Irache JM, Peñuelas I. Radiolabeling and biodistribution studies of polymeric nanoparticles as adjuvants for ocular vaccination against brucellosis. Rev Esp Med Nucl Imagen Mol. 2013 March; 32 (2): 92–97.
[11] Langer K, Balthasar S, Vogel V, Dinauer N, von Briesen H, Schubert D. Optimization of the preparation process for human serum albumin (HSA) nanoparticles. Int. J. Pharm. 2003 May; 257 (1-2): 169–180.
[12] Sing N, Lewington V. Molecular radiotheragnostics in thyroid disease. Clin Med (Lond). 2017 October; 17 (5): 453-457.
[13] Griffin N, Grant LA. Endocrine system. Churchill Livingstone. 2013: 856-871.
[14] Williams JG, Croft DN. Carbenoxolone and gastric Technetium-99m pertechnetate uptake in patients with gastric ulceration. Scand J Gastroenterol Suppl. 1980; 65: 29-33.
[15] Harvey A, Ziessman MD, Janis P, O'Malley MD, James H, Thrall MD. Chapter 11 Gastrointestinal System. Nuclear Medicine (Third Edition). 2006: 346-383.
[16] Neels OC, Kolenc P, Patt M. Ions and small molecules as radiopharmaceuticals. Biomedical Sciences. 2021.
[17] Dittrich RP, De Jesus O. Gallium Scan. StatPearls. 2022.
[18] Birn H, Christensen EI. Renal albumin absorption in physiology and pathology. Kidney international. 2006 February; 69 (3): 440-449.
[19] Comper WD, Osicka TM, Russo LM. Renal Filtration, Transport, and Metabolism of Albumin and Albuminuria. Seldin and Giebisch's The Kidney (Fourth Edition). 2008; 2: 2081-2112.
[20] Kazazi-Hyseni F, Beijnen JH, Schellens JHM. Bevacizumab. Oncologist. 2010 August; 15 (8): 819-825.
[21] CheMaTech. p-NCS-benzyl-NODA-GA. [Internet]. Available from: https://www.chematech-mdt.com/produit/p-ncs-benzyl-noda-ga/. [Accessed: 25-05-22].